Istituto Nazionale di Oceanografia e di Geofisica Sperimentale (Trieste, ITALY)

PEGASOS Project

ESTIMATION OF THE MEDIAN, NEAR FAULT GROUND MOTION IN SWITZERLAND.

SCIENTIFIC REPORT N. 6

Enrico Priolo[(1)], Alessandro Vuan[(1)], Peter Klinc[(1)], and Giovanna Laurenzano[(2,1)]

[(1)] *Istituto Nazionale di Oceanografia e di Geofisica Sperimentale (Trieste) – Seismological Research Centre Department (Udine), Italy*

[(2)] *Dipartimento di Ingegneria Civile - Università degli Studi di Trieste*

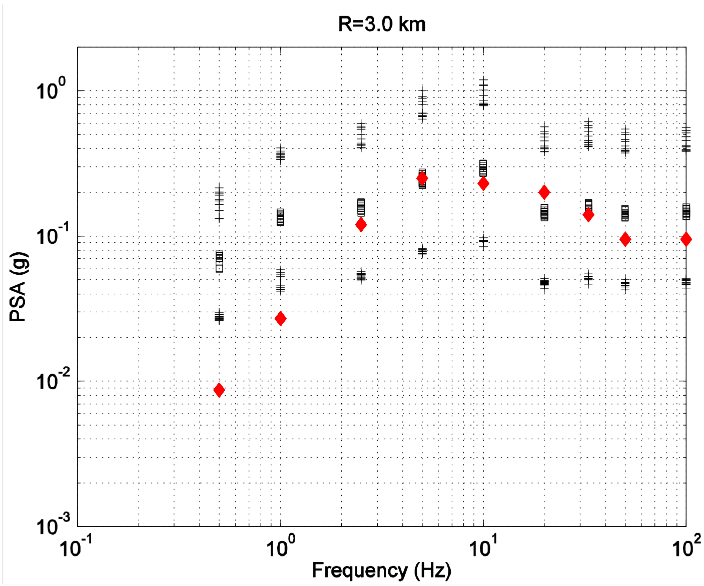

Scientific responsible: Dr. Enrico Priolo

Director of CRS Department: Dr. Alberto Michelini

Rel. OGS-27/2003/CRS-3
June 30th, 2003

Introduction

The spectral acceleration assessed by the OGS simulations (Priolo et al., 2003) are generally larger that those estimated by the SP2 experts (see for instance, Figure 1). In particular, the OGS low frequency pseudo-spectral acceleration (i.e at frequencies 1 and 0.5 Hz) features higher amplification and smoother decay. We are convinced that our method provide reliable results in that band. This was also confirmed by Madariaga (2002) who reported that "both OGS and URS approaches are interesting and well constructed at low frequencies and match very well the results of rupture dynamics". Here we investigate the possible reasons of the low decay predicted at low frequencies by the OGS simulations and propose some actions to better interpret or integrate those results.

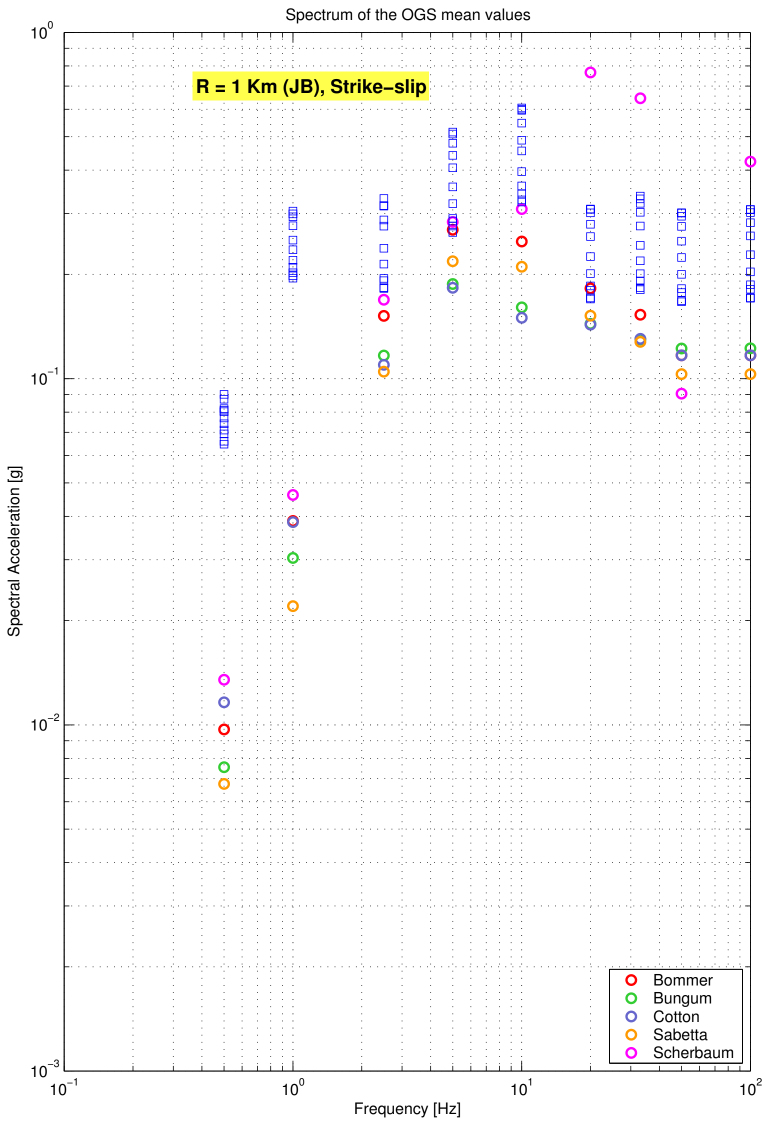

Figure 1: Spectral pseudo-acceleration estimated by the SP2 experts (circle marks) and OGS (square marks) at distance R = 1 km for strike-slip mechanism. By courtesy of Philippe Roth.

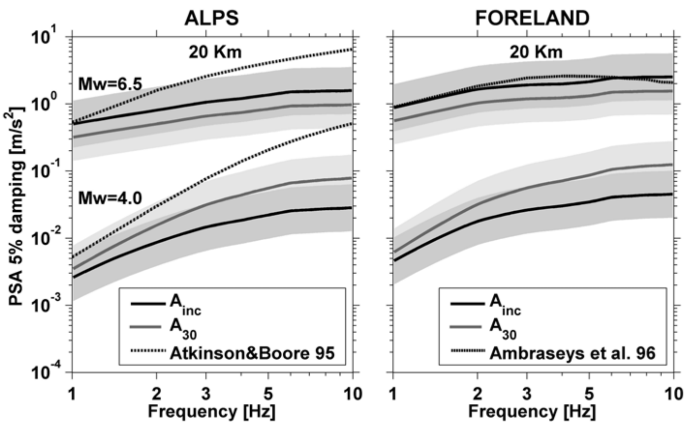

Figure 2: Spectral pseudo-acceleration (5% damping) at 20 km of hypocentral distance estimated by Bay et al. (2002). Modified from Bay et al. (2002).

Analysis and Discussion

First we have compared our estimates to those provided by Bay et al. (2002) for Switzerland. Figure 2 shows their estimates for the Alpine and Foreland models, corresponding to a NEHRP A and NEHRP B soil classification, respectively. The curves estimated for magnitude 6.5 have a gentle slope, and the values are contained well within one decade for all frequencies. They agree more with that estimated by OGS than those provided by the SP2 experts. Note that the Bay's "Foreland" model, corresponds to a NEHRP B site, i.e. 30 m thick soft rock (750 m/s $< V_S <$ 1500 m/s), while for CHN model the soft rock layer is considerably thicker (150 m). This can explain the higher amplification in the low frequency band we obtained by using the CHN model.

The pseudo-spectral acceleration (PSA) decay at frequencies lower than 2 Hz can be influenced by the following factors: 1) the structural model, 2) the shape of the k^{-2} slip distribution and 3) directivity. Below we discuss on how these factors can affect the PSA shape.

1) The CHN model produces a resonant peak at 2.1 Hz due to the 150 m thick shallow layers. The effect of this structure is clearly shown in Figure 3 (blue line) and shows up as a strong surface wave train in the point source seismograms, whose amplitude and duration depends on the source-receiver distance. The surface wave train disappears completely in a hypothetical "rock" model with the "seismogenic" layer ($V_S = 3.6$ km/s) extending up to the surface (red line, in Figure 3). The maximum simulated frequency is $f_{max} = 2.5$ Hz. In the response spectrum, the model CHN produces a large peak of amplification in a band around 2 Hz, and a somewhat weaker peak at lower frequencies in the band 0.2-0.7 Hz.

2) The slip distributions used in (Priolo et al, 2003) cover the fault area (Figure 4)

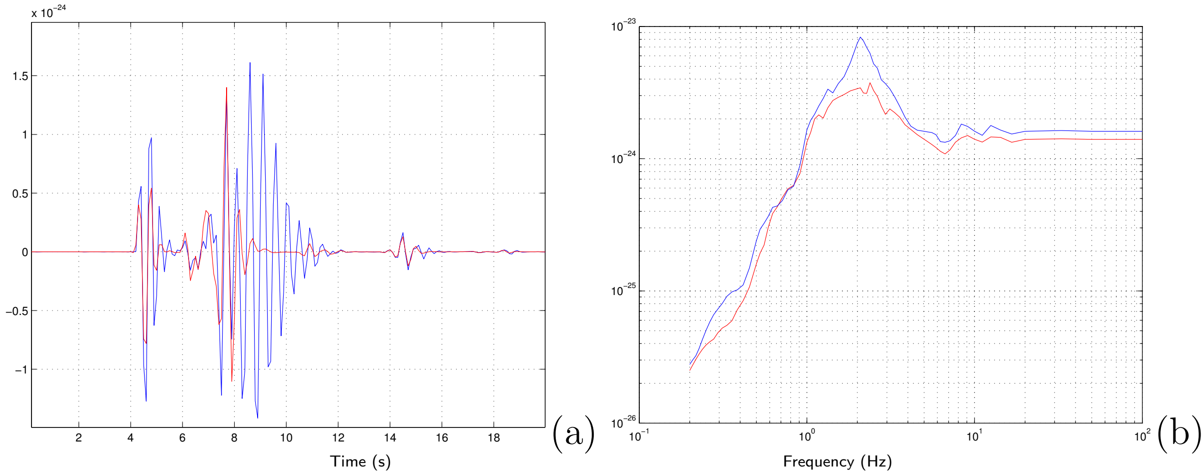

Figure 3: Acceleration seismogram (a) and response spectra (b) computed for model CHN (blue curve) and an equivalent rock model (red curve). The maximum represented frequency is $f_{max} = 2.5$ Hz. See text for further details. The source is a strike-slip point source located at depth of 7 km (i.e., source n. 5 in Figure 2 (Priolo et al., 2003)). The receiver is located at distance R = 25 km, nearly along strike (i.e., site n. 11 in Figure 4 (Priolo et al. (2003)).

almost uniformly. In particular, the non-null area of slip have rather regular and sharp boundaries, so that one can clearly distinguish few compact asperities, which in some cases may fulfil the whole area. Regular boundaries have the effect of increasing the low frequency seismogram amplitude, as is shown in Figure 5, where the seismograms, computed using both distribution n. 1 of (Priolo et al, 2003; black line) and a homogeneous slip distribution over the whole fault (blu line), feature an overall similar shape with a common dominant frequency of about 1 Hz.

We observe that the boundary segmentation of the slip distribution plays a relevant role in building up the frequency content of the computed seismograms. Therefore, we have created a new set of five k^{-2} distributions with more irregular boundaries (Figure 6). The resulting seismogram (red line) features a higher dominant frequency (see Figure 5).

Figures 10-14, show the statistics of the spectral accelerations obtained with both the new and previous set of slip distributions, respectively. In general, the new set of results display higher amplitudes (except for $R = 1$ km), smoother trends, and fit slightly better the estimates of the SP2 experts. The low frequency band (i.e., $f < 2$ Hz) still features amplification, which we interpret as mainly due to the considered structural model .

We have no enough experience to claim that this last data-set of slip distributions is more realistic than the previous one. We leave to the SP2 experts the choice of which one to prefer or enter into the statistics.

3) In order to analyze the effects of directivity, we define two profiles of nucleation points aligned along fault strike and dip, respectively (Figures 7). Figures 8 and 9 show the seismograms obtained at receiver n. 11 for the two set of nucleation points. We

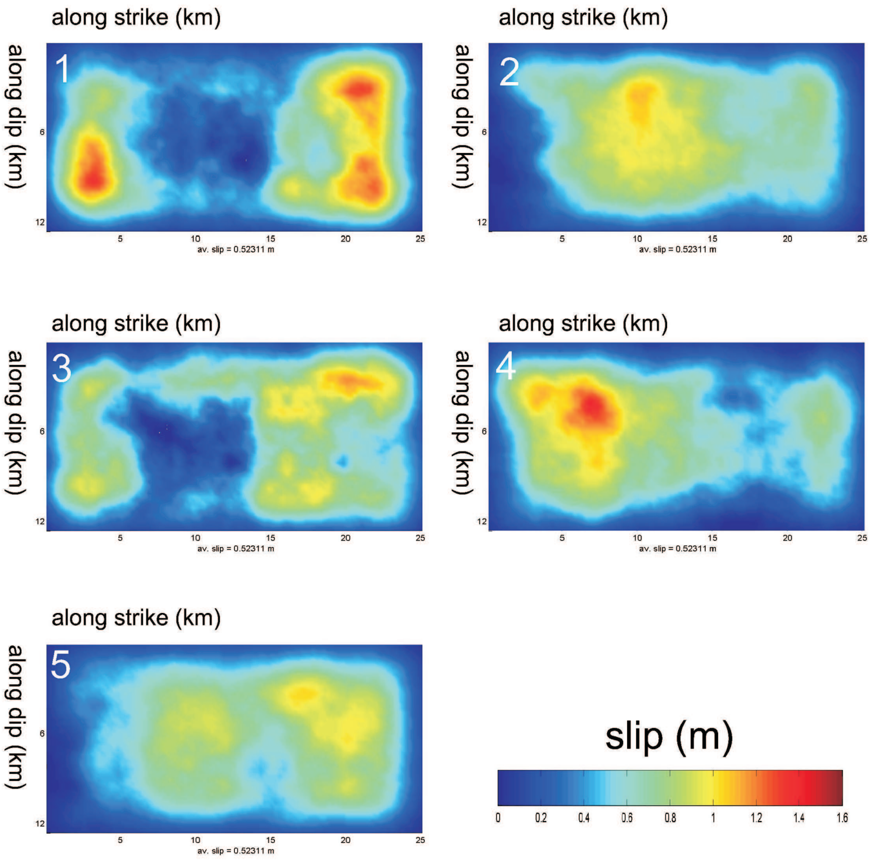

Figure 4: The five slip distributions used in (Priolo et al., 2003).

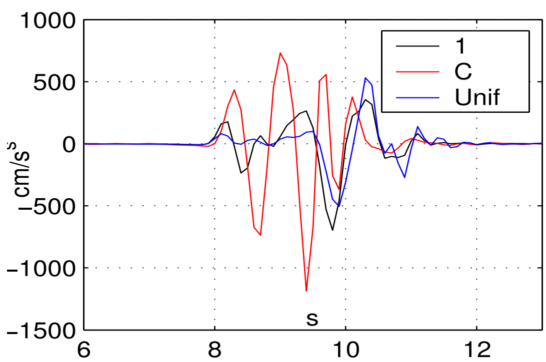

Figure 5: Seismograms computed for different slip distributions, i.e. distribution n. 1 of Priolo et al (2003) (black curve), a uniform slip distribution (blue), and distribution C of this report (red).

restrict the discussion to the strike-slip mechanism and consider only the frequency band up to $f = 2.5$ Hz. North and East components of pseudo-spectral acceleration display similar behavior for both the horizontal and down-dip nucleation alignments, although the overall amplitude varies between them. For the set of nucleations aligned along strike (Figure 8), the larger the directivity the steeper is the PSA low frequency slope (i.e., for $f \leq 1$ Hz) and the more pronounced is the "bump" in the band 1-2.5 Hz. As directivity

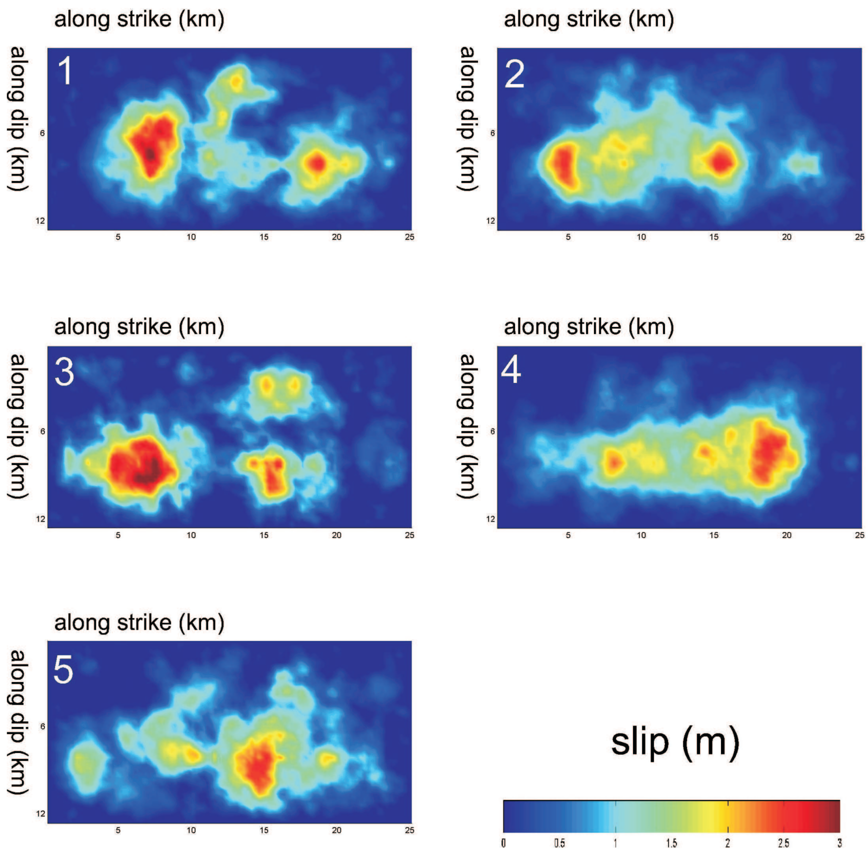

Figure 6: The new five slip distributions used in this report.

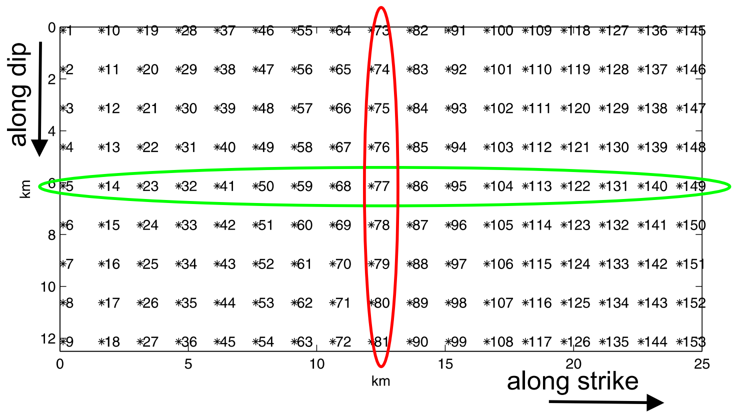

Figure 7: Geometry of the nucleations used to evaluate the effect of directivity along strike (green ellipse) and dip (red ellipse).

decreases, the slope becomes lower and the PSA bump shows up at lower frequency. For the set of nucleations aligned along dip (Figure 9), the directivity shows again up with the "bump" at 1-2.5 Hz, however it does not affect the low frequency slopes of the spectra. Note that the variability of the estimates is very small in the low frequency band while it increases at frequency higher than 1 Hz.

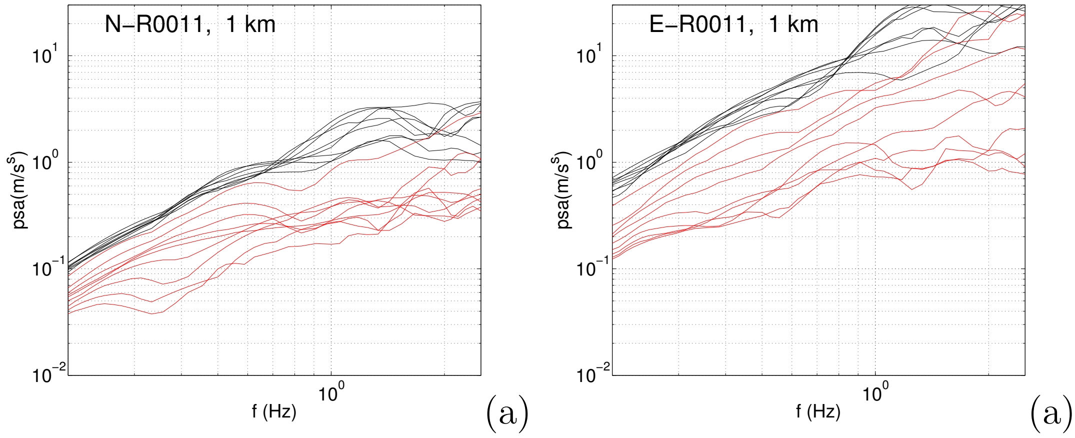

Figure 8: Acceleration response spectra computed for strike slip mechanism at receiver n. 11 for a set of nucleations aligned along fault strike (see Figure 7). The black and red curves show the spectra computed for directive and anti-directive rupture propagations, respectively. (a) North component; (b) East component.

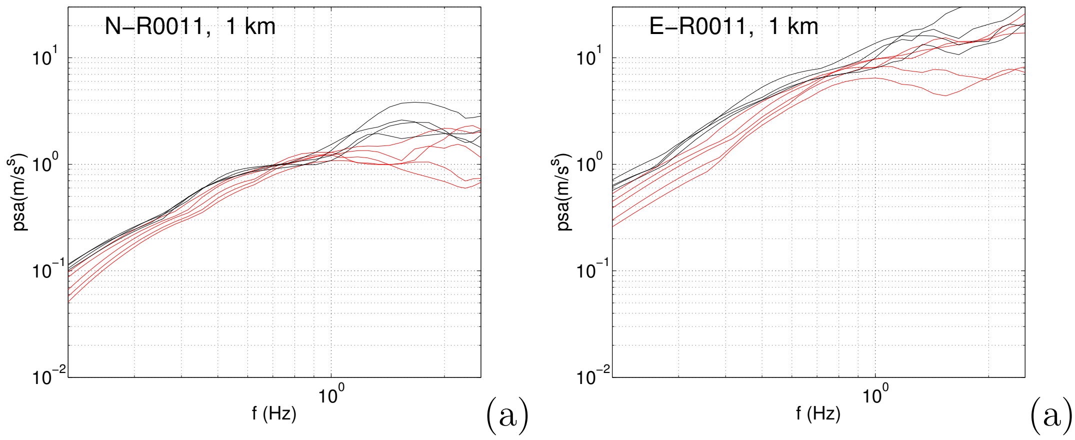

Figure 9: Same as Figure 8 but for nucleations aligned along dip.

Conclusions

A new set of simulations has been computed to interpret the differences encountered in matching SP2 experts estimations of PSA. In our opinion, the amplification of the low frequency band (i.e., $f < 2$ Hz), which shows up in our simulations, have to be addressed to the CHN model. This model can be considered representative of a NEHRP B class soil, but with a considerably thicker shallow velocity layer (150 m). The resulting amplification should be accounted for in hazard estimations and, on average, it can be considered typical of the Swiss Foreland region. We have also shown that our estimates agree with those provided by Bay et al., (2002), which found the same nearly flat decay of PSA at low frequencies.

We have shown that some additional factors influence, as a second order effect, the response in the low frequency band. As an example the areal shape of slip distribution, in the sense that rectangular boundaries do increase the low frequency amplitude. In our previous set of simulations (Priolo et al., 2003), the slip distribution samples the rectangular fault plane almost uniformly. We interpret that the coherent signal coming from the rupture propagation along the fault boundaries contributes in some way to increase the spectral pseudo-acceleration amplitude in the band below 2 Hz. Consequently, we have defined and used a new set of distributions with segmented boundaries, which provide a new set of results. We have no elements to address which one of the two sets of slip distributions is more realistic.

1 References

Bay, F. (2002). Ground motion scaling in Switzerland: Implications for Hazard Assessment. Ph. D. Thesis, ETH, Zurich, 98 pp. + Appendices.

Madariaga, R. (2002). Assessment of feasibility of kinematic fault models used for upper limit ground motion evaluations for the Pegasos project. Pegasos Project, Technical Note n. EXT-TN-0308, 8 pp.

Priolo, E., Vuan, A., Klinc, P., and Laurenzano, G. (2003). *PEGASOS Project — Estimation of the median, near fault ground motion in Switzerland. Scientific Report n. 5* Report n. OGS-21/2003/CRS-2. Borgo Grotta Gigante, July 10, 2003. 30 pp.

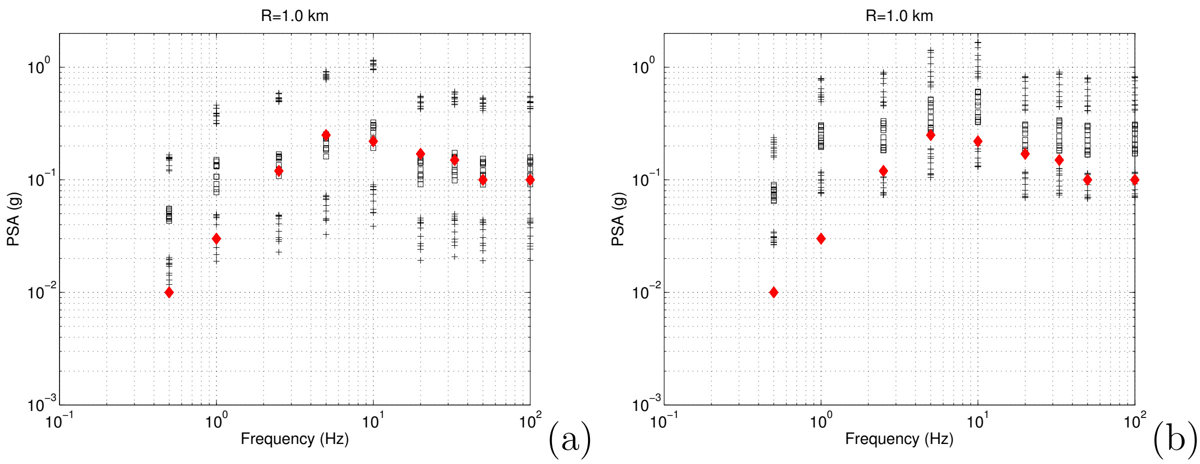

Figure 10: Spectral pseudo-acceleration (5% damping) obtained at distance $R = 1$ km. The square and cross marks represent the median and median plus/minus the first standard deviation (one triplet of marks for each receiver) obtained considering the two mechanisms, all nucleations, and five slip distributions. Values obtained using (a) the new distributions A-D of Figure 6, and (b) distributions 1-5 used in the previous report (Figure 4). The red diamonds represent the median of the values provided by the SP2 experts and visually estimated by the authors from the figures provided by Philippe Roth.

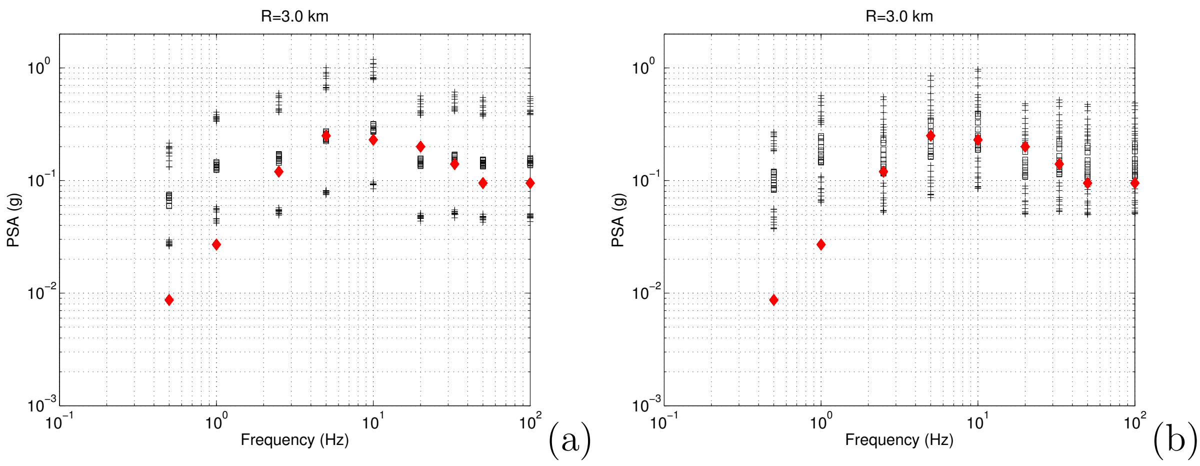

Figure 11: Same as Figure 10, but at $R = 3$ km.

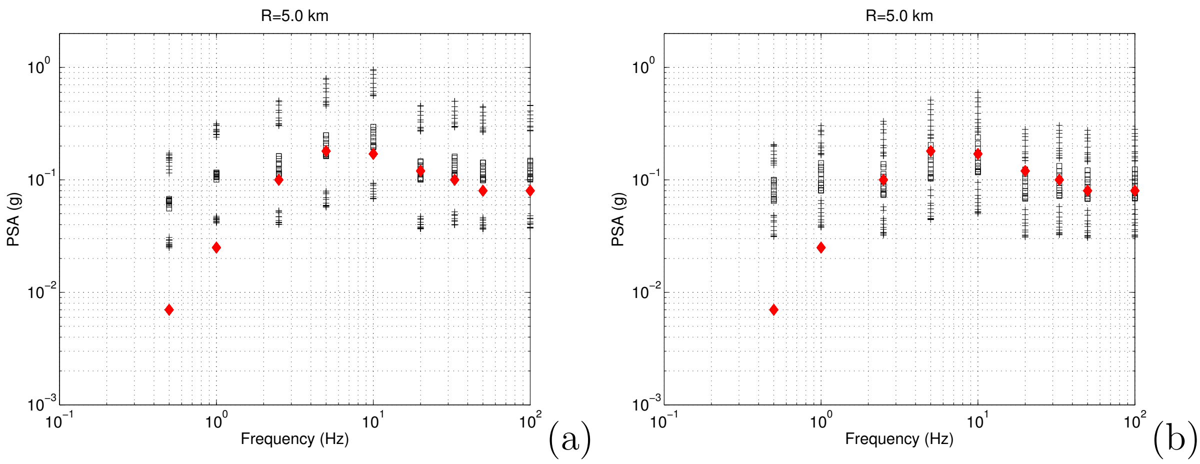

Figure 12: Same as Figure 10, but at $R = 5$ km.

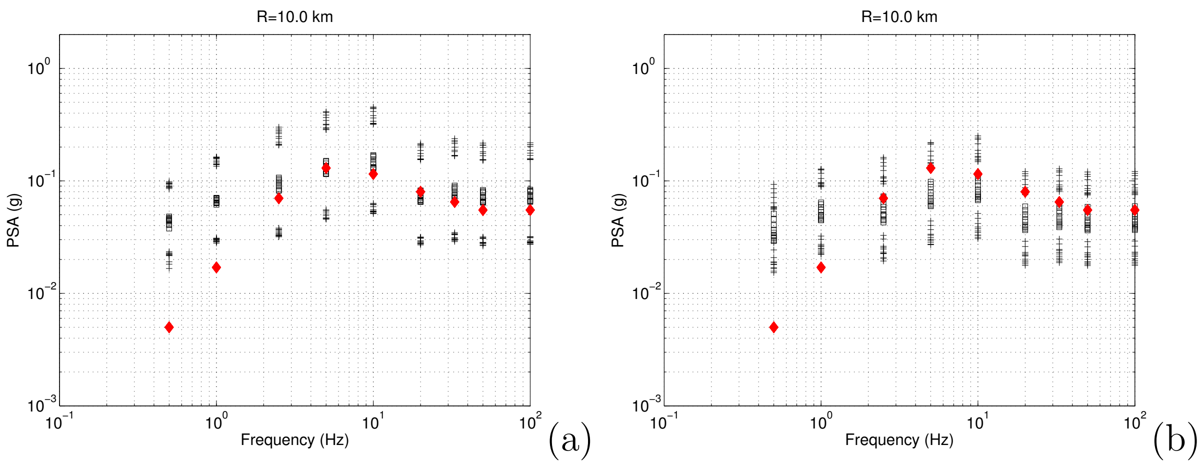

Figure 13: Same as Figure 10, but at $R = 10$ km.

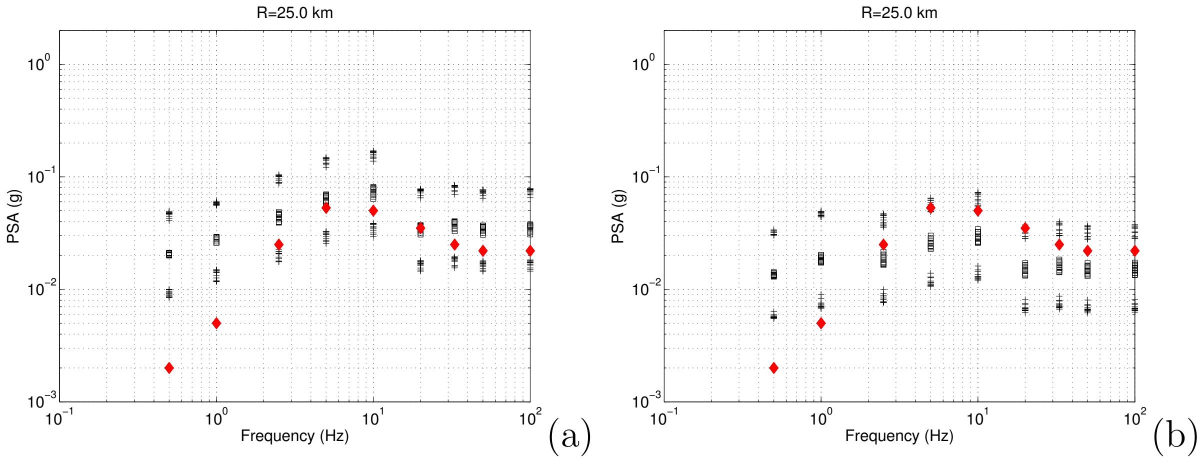

Figure 14: Same as Figure 10, but at $R = 25$ km.